C. R. Mecanique 342 (2014) 264–272

Contents lists available at ScienceDirect

Comptes Rendus Mecanique

www.sciencedirect.com

Frontiers of micro and nanomechanics of materials: Soft or amorphous matter, surface effects

Mechanics of network materials with responsive crosslinks

Chao Wang [a,b], Enlai Gao [a], Lifeng Wang [c], Zhiping Xu [a,*]

[a] *Applied Mechanics Laboratory, Department of Engineering Mechanics and Center for Nano and Micro Mechanics, Tsinghua University, Beijing 100084, China*
[b] *Institute of Advanced Study, Nanchang University, Nanchang, China*
[c] *Department of Civil and Environmental Engineering, Clarkson University, Potsdam, NY 13699, USA*

ARTICLE INFO

Article history:
Received 4 June 2013
Accepted 1 December 2013
Available online 9 May 2014

Keywords:
Networked materials
Mechanical properties
Responsive materials
Dynamic materials
Crosslinks

ABSTRACT

The mechanics of responsive fiber-network materials have been explored here by performing coarse-grained molecular dynamics simulations. Theoretical analysis based on a simple viscoelastic model is used to characterize the relationship between their microstructures and overall mechanical behaviors. The dynamic responses in stress and strain induced by externally tuned interfiber crosslinks are discussed. Our results here indicate the possibility of optimizing the dynamic performance of macroscopic network materials by tuning the crosslinks at the molecular level, and lay the groundwork for dynamic material design for structural and mechanical applications.

1. Introduction

Natural and engineering materials featuring hierarchical structures have attracted much interest recently for the rational design of structural and functional materials and the understanding of their structure–property relationship [1,2]. Examples of these materials include fiber-network membranes for filtration and separation uses [3], structural and functional nanocomposites [4], as well as biological materials (e.g., cytoskeleton networks [5], spider webs [6]). The microstructure of these materials features multiple length scales and gives rise to complicated behaviors that remain to be understood. The other side of the coin is that they offer great tunable and controllable material properties. This concept of dynamic (e.g., responsive, self-healable, reversible, active) materials and performance was widely discussed recently, especially for bio-inspired synthetic materials [7–9].

Networked materials constructed from micro and nanofibers with dynamic interfaces between them serve as excellent examples of the aforementioned concept and platforms to explore structure–property relationship. Dynamical crosslinks between synthetic polymers, such as hydrogen bonds and metal–ligand coordination complex, feature responsive and active mechanical properties [10]. The cell, with cytoskeleton fibers as the scaffold, presents an integrated example of highly nonlinear materials with dynamic responses to chemical and mechanical cues [5]. From the point of view of engineering, the concept of dynamic properties of materials, especially the stimuli-responsive behavior, holds great promise in broad applications such as robotics, actuators, artificial muscles, and tissues. A representative structure of typical networked materials is illustrated in Fig. 1a. Fibers are connected through strong (e.g., chemical bonds, etc.) and/or weak (e.g., van der Waals interactions, hydrogen bonds, etc.) crosslinks. Synthetic polymers have been widely used in responsive materials where the deformation and mechanics are dominated by the entropic elasticity [10–12]. Attention was paid to the role of dynamic

* Corresponding author.
E-mail address: xuzp@tsinghua.edu.cn (Z. Xu).

http://dx.doi.org/10.1016/j.crme.2014.03.005
1631-0721/

Table 1
Simulation parameters used in the crosslinked CNT network model [13,14,20].

Parameters	Values
Equilibrium bead distance R_0 (Å)	10
Tensile stiffness parameter K_T (kcal mol^{-1} Å^{-2})	500
Equilibrium angle θ (°)	180
Bending stiffness parameter K_B (kcal/mol)	14 300
Van der Waals parameter ε (kcal/mol)	15.1
Van der Waals parameter σ (Å)	9.35

crosslinks, or dynamic bonds in constructing materials with environmental responsiveness [9]. Recent studies have shown that these adaptive systems have the potential to revolutionize technologies such as sensors, actuators, and biomedical applications [9]. One further step from this point is that supermolecular fibers with outstanding physical properties could be used instead of the polymers traditionally chosen to further elevate the dynamic material performance. For example, our previous work has suggested that carbon nanotubes (CNTs)-based networked materials feature not only promising mechanical performance as structural materials, but also tunable structures and properties, while crosslinks, strong or weak, are introduced at their interfaces [13,14]. It should be noted that the persistence length of a CNT is on the order of 10–100 μm [15], and mechanical responses of these semiflexible networks are expected to be more significant than flexible polymers where entropic elasticity controls.

To formalize the mechanics of crosslinked semiflexible fiber networks, efforts have been made to explore the static and dynamical performance of a representative unit of crosslinked fibers [16,17]. Model for active gels and responsive networks were developed based on single mechanical units [18,19]. Network-level studies have been carried out using molecular dynamics simulations, usually at a coarse-grained level [13,14]. In this work, we provide a synergetic description of the network by considering properties of all building blocks (fibers, crosslinks) and establish a correlation between the microstructures and overall mechanical properties at the network level, focusing on their dynamic responses to environmental cues.

2. Materials and methods

2.1. The coarse-grained model

We adopted a coarse-grained description of CNTs to access time and spatial spans over 100 ns and 1 μm, which was used earlier in studies of CNT networks with van der Waals interfaces [11,12,15]. In this model, discrete beads interacting through bond and angle springs provide a description equivalent to the continuum mechanics model with specific tension stiffness, bending rigidity, and intertube binding energy. Within each nanotube, the stretching contribution between two bonding beads with distance R to the total energy is given by $E_T = K_T(R - R_0)^2$, where $K_T = YA/R_0$ is the spring constant relating to the tension stiffness, expressed using the Young modulus Y, the cross-section area A, and the equilibrium distance R_0. The bending energy contribution within adjacent beads triplets is described as $E_B = K_B(1+\cos\theta)$, where $K_B = 2YI/R_0$ is the angular spring constant relating to the bending stiffness $D = YI$ and θ is the bending angle within the triplet. D is calculated by fitting results from full-atom MD simulations. I is the bending moment of inertia. In addition, we define the van der Waals interactions between beads in different CNTs by the 12-6 Lennard-Jones formula $E_{vdW} = 4\varepsilon[(\sigma/R)^{12} - (\sigma/R)^6]$. These parameters are summarized in Table 1.

In addition to the van der Waals interactions between the fibers, we added crosslinks by using a table-defined potential function, which allows us to describe the breakage and formation of crosslinks, i.e. the reactivity. The stiffness and strength of the crosslinking interaction were fitted to the values obtained from first-principles calculations [21]. These settings for the crosslinking mechanics are representative in this study and could be extended to other forms of chemical or physical interactions. In the discussion on responsive mechanics of CNT networks, a harmonic bond interaction was used instead, with the same stiffness as the reactive one. The spatial distribution of these crosslinks is uniform in the network sample, by bonding to a pair of beads (binding sites) in two neighboring fibers.

2.2. Sample preparation in simulations

A two-dimensional periodic boundary condition was used in both in-plane directions x and y. The length L and width W of the periodic simulation box are 0.12 and 0.07 μm, respectively. (5, 5) CNTs with a contour length of 100 nm were firstly constructed with an initial curvature defined by the thermal fluctuation amplitude, and then deposited layer by layer. The orientations of CNTs were uniformly distributed between 0 and π before the deposition. The microstructures of the CNT network and the dimensions of the periodic simulation box were equilibrated by integrating the Langevin equations of motion before mechanical loads were applied. To accelerate the equilibrium process, a body force was initially applied and a rigid supporting substrate was added below to make the whole structure more compact, following closely the procedures conducted in experiments [22]. After that, the force and substrate were both removed to maintain the membrane's structure. A Langevin thermostat at 300 K was applied for one microsecond till the fluctuation of total energy converges below 0.1%.

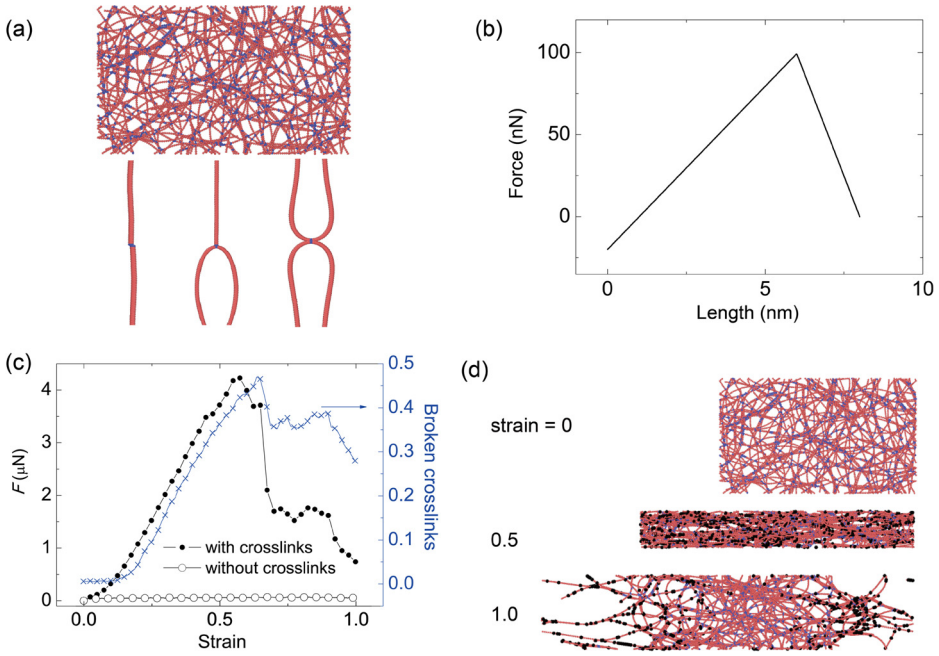

Fig. 1. (Color online.) (a) A simulation snapshot of network material microstructures with crosslinked interfaces (blue beads) between fibers (red chains) illustrated in the insets. (b) The force–length relation used in the simulation for a single crosslink. (c) A typical tensile force–strain relationship of the network material, showing the effect of covalent crosslinks on overall mechanical performance. (d) Simulation snapshots showing the material fracture processes at different strain levels, as defined by the breakage of crosslinks. Black (blue) beads represent binding sites in the fibers, where the crosslinks are (not) broken. (For interpretation of the references to color in this figure, the reader is referred to the web version of this article.)

Due to the relatively large supercell used for the network here in our simulations, the distributions of intratube bond distances and angles are isotropic in the x and y directions. The thickness h of a CNT network in our simulations was defined as the maximum spatial extension in the z direction of the sample. We prepared several samples with varying initial carbon nanotube densities n. The mass density ρ of the CNT network increases with the thickness of deposited materials in the beginning and then converges at the equilibrium density in ambient conditions, i.e. 0.28 g/cm^3 for $h = 9$ nm. This value of mass density is close to that reported for single-walled buckypapers [23,24]. It should be noted that due to the highly inhomogeneous microstructure of the material, we will refer to the internal force across the material rather than to stress on load transfer in the following discussions.

2.3. Molecular dynamics simulations of mechanical loading

A tensile load was applied by deforming the simulated supercell. The loading rate v is 3 m/s. Simulations at a lower loading rate ($v = 0.1$ m/s) were also carried out and the rate dependence is found to be negligible. The equations of motion were integrated using a velocity Verlet algorithm with a time step of 10 fs that ensures the numerical convergence of integration. The pressure in the transverse y direction was restrained as zero during the uniaxial tensile loading process by using a Berendsen barostat. For equilibration in a pre-stress condition, a Langevin thermostat and Berendsen barostat was coupled to relax both the sample configuration and the dimensions of the periodic simulation box, while for equilibration in pre-strain conditions, the network structure was relaxed in a Langevin thermostat and a fixed simulation box.

3. Results

3.1. Deformation and fracture of crosslinked networks

The microstructures of crosslinked CNT network obtained after equilibration are plotted in Fig. 1a, with three characteristic crosslinking subunits illustrated in the insets. The crosslinks (highlighted by blue color) are randomly distributed in the material with a density of 10.7 crosslinkers per fiber, connecting acceptors and donors in different fibers. The interfiber interaction established by a crosslink is assumed to be pairwise, i.e. depending on the distance between acceptor and donor binding sites only. This interaction drops to zero at a large distance and could recover once the crosslinking pair sites re-enter their interacting range. The tensile force–strain dependence of a single crosslink is plotted in Fig. 1b. In experiments, the crosslinks could be realized through covalent bonds, coordination complex, cooperative hydrogen bonds, etc. Without loss of generality, we use a model crosslink here with a relaxed length of 1 nm. The tensile stiffness of the crosslink is

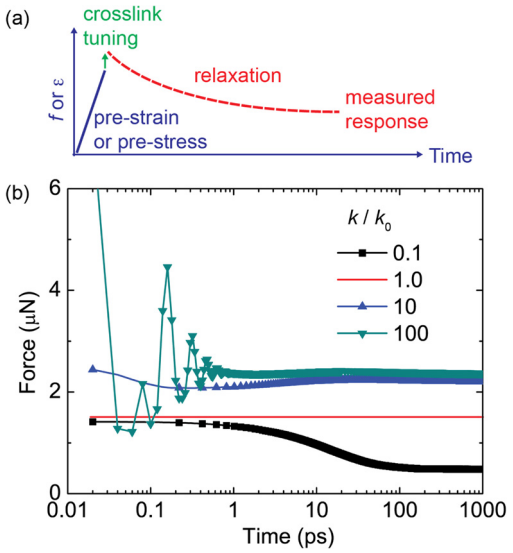

Fig. 2. (Color online.) (a) Illustration of the simulation procedure, where prestress or prestrain was applied to the relaxed structure, followed by crosslink tuning and relaxation of network microstructure. The response in force or strain was measured after a plateau of the measured value was reached. (b) Responses in the tensile force at a prestrain of 0.25, when the stiffness of crosslink is modified from k_0 to k.

19.8 N/m and a peak force of 99.2 nN is set at $d = 6$ nm. This crosslink is much softer and more resilient than the fibers and thus under mechanical loads non-affine deformation modulated by stretching the crosslink is expected.

The mechanics of crosslinked networks was explored under uniaxial tensile loads. The force–strain relationship thus obtained is summarized in Fig. 1c. The mechanical behavior is determined by the performance of both the network elasticity and crosslinks, including contributions from stretching, bending, and intertube interaction [13]. Comparing the results for CNT networks with and without covalent crosslinks, it was found that mechanical enhancement with ~58 times higher strength is established by crosslinking CNTs because the original van der Waals interaction between CNTs is rather weak, which cannot resist intertube sliding and detachment, which corresponds to the plateau in the force curve and leads to ductile material failure. In contrast, for the crosslinked network, the tensile force reaches the maximum at a strain of 0.57. The crosslinks start to break extensively afterwards, and the crosslinked nature of the CNT network is destroyed.

The simulation snapshots in Fig. 1d at uniaxial tensile strains of 0.5 and 1.0 show the microstructures of a CNT network before and after the crosslinks connecting them are broken, successively. The simulation results show that fracture of the network nucleates locally, followed by catastrophic breaking of crosslinks in that region. The percentage of broken crosslinks N_C corresponds to distinct behaviors in the force–strain relationship. N_C is almost zero at the initial loading stage ($\varepsilon < 0.1$). It gradually increases at larger strain up to 46.9%, with a linear dependence on the strain for $\varepsilon < 0.65$, indicating spreading of crosslink fracture within the material. After the main fracture zone forms ($\varepsilon > 0.65$), some crosslinks start to be recovered within the relatively intact region of the material, corresponding to a reduction in N_C from 46.9% to 37.5%. For $0.7 < \varepsilon < 0.9$, the external tensile load is withstood by shear resistance between fibers and there are no more breakage or recovery events observed for the crosslinks. At $\varepsilon > 0.9$, due to the topological changes in the network facilitated through interfiber sliding, progressively reduced shear resistance between the fibers is observed and more crosslinks in the intact region are self-healed.

3.2. Responsive crosslinks

From the previous discussion, we can see that the interfiber crosslink plays a dominant role in modulating the deformation and failure behaviors of the network. Moreover, network materials with responsive crosslinks could also behave dynamically in an active environment. Following the discussion above on the crosslinking effects in tuning material properties of CNT networks, we focus in this section on their dynamic responses when the crosslinks are modified. The strength k and the equilibrium position r_0 are two key controlling parameters for a crosslink at equilibrium, whose energetic description is approximated as a harmonic function $E = k(r - r_0)^2$ here, where r is the distance between the binding sites of the crosslink. Upon dynamic stimulations, parameters k and r_0 could be modified, which consequently leads to changes in the network structure and stress field therein. The response depends on the boundary conditions, i.e. whether the network is in a state of pre-applied strain or stress. The simulation procedure is illustrated in Fig. 2a.

3.2.1. Responses in a pre-strained network

We firstly discuss here the change in tensile force transferred across the material by tuning the strength k and the equilibrium position r_0 of crosslinks, at a finite pre-strain $\varepsilon_0 = 0.25$. The choice of this relatively large strain is made to magnify

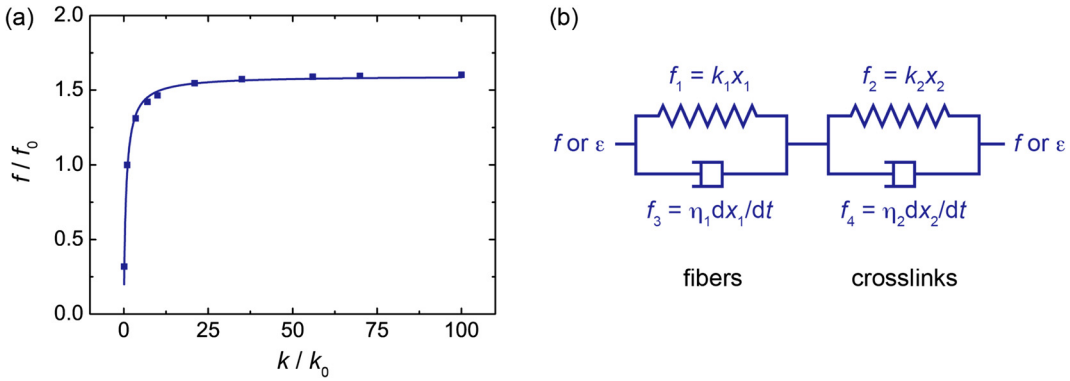

Fig. 3. (Color online.) (a) Response in tensile force f/f_0 measured as a function of the stiffening factor k/k_0; (b) A generalized Kelvin–Voigt model characterizing the viscoelastic behavior of crosslinked networks investigated here in the simulations, where $x_{1,2}$ is the change in length of each Kelvin–Voigt unit.

the observed response in our simulation. The complicated material behaviors such as breaking of crosslinking nature, reorientation, bundling of fibers (CNTs bind to each other and form thick bundles), and interfiber sliding as observed in our simulations [13,14] are not discussed here, and are precluded by our harmonic approximation of crosslinking mechanics in following discussions.

Stiffness. The simulation results on the response in tensile force f after modifying the stiffness of crosslinks by changing k_0 into k are shown in Fig. 2b, compared with the load transfer in the original network f_0. k_0 was set to 10 N/m in our simulations. It is suggested by the results that the tensile force changes promptly after the modification, and slowly relaxes into a constant after a time scale of a few picoseconds for stiffening ($k/k_0 = 10$) and ~100 ps for softening ($k/k_0 = 0.1$). For large stiffening factors (e.g., $k/k_0 = 100$), strong oscillation is observed in the amplitude of the tensile force during the relaxation process. The relaxation of the force amplitude corresponds to the microstructural adjustment of the CNT network, including deformation of CNTs and changes in the network structure. The length of crosslinks contracts accordingly when their stiffness is enhanced and extends vice versa. This can be explained by the force balance between the crosslinks and the CNT.

The response in tensile force is further measured here by the relative amplitude f/f_0, as plotted in Fig. 3. The results show more prominent effects in the response when the crosslinks are softened ($k/k_0 < 1$) than when they are stiffened ($k/k_0 > 1$). The responsive mechanics of a pre-compressed network is more complicated, as buckling of the slender fibers would bring in additional relaxation modes as the crosslinks are modified, which will not be discussed here.

To characterize the simulation results presented in Figs. 2b and 3a, we construct a generalized Kelvin–Voigt model here as illustrated in Fig. 3b. The two sets of springs and dashpots represent the viscoelasticity of the crosslinks and CNTs, respectively. At a pre-strain of 0.25, there is no evidence from the simulation results of crosslink breakage or non-affine deformation, as the harmonic approximation is applied for crosslinks. Thus in the spirit of affine deformation approximation, which is valid before significant topological change occurs, this simple model is expected to be able to predict the mechanical behavior of the crosslinked network.

By introducing the key parameters k_1, k_2 and η_1, η_2 for the generalized Kelvin–Voigt model (Fig. 3b), the model could be used to fit these parameters from simulation results. In this model, when the material is pre-stretched at a strain ε_0 or an extension x, we have:

$$x = x_1 + x_2 = L\varepsilon_0 \tag{1a}$$

$$f = f_1 + f_3 = f_2 + f_4 \tag{1b}$$

where f_1 and f_2 (f_3 and f_4) are the forces in the two sets of springs (dashpots) respectively. By solving Eq. (1) with $f_3 = \eta_1 \mathrm{d}x_1/\mathrm{d}t$ and $f_4 = \eta_2 \mathrm{d}x_2/\mathrm{d}t$, we have:

$$f = k_1 k_2 L\varepsilon_0/(k_1 + k_2) \tag{2}$$

at the limit when t approaches infinity, where $L = 0.12$ μm is the original length of the sample. In the generalized Kelvin–Voigt model, k_1 and k_2 are the stiffness of the CNT network and the crosslinks, and $k_2 = \alpha k$. A scaling parameter α is used to include the effective contribution from all crosslinks from the whole sample. k is the stiffness of a single crosslink. As shown in Fig. 3a, Eq. (2) fits well the simulation results, and the parameters thus obtained are $k_1 = 80$ N/m and $\alpha = 6$. Thus, as k is 10 N/m, the stiffness of the material $k_{\mathrm{eff}} = k_1/(1 + k_1/k_2) = 34.3$ N/m. It should be noticed that k_1 is contributed from both stretching and bending deformation of the CNTs.

The time-dependent response in force as shown in Fig. 2 can be explained by using an effective damped oscillator model for the whole material with the equation of motion:

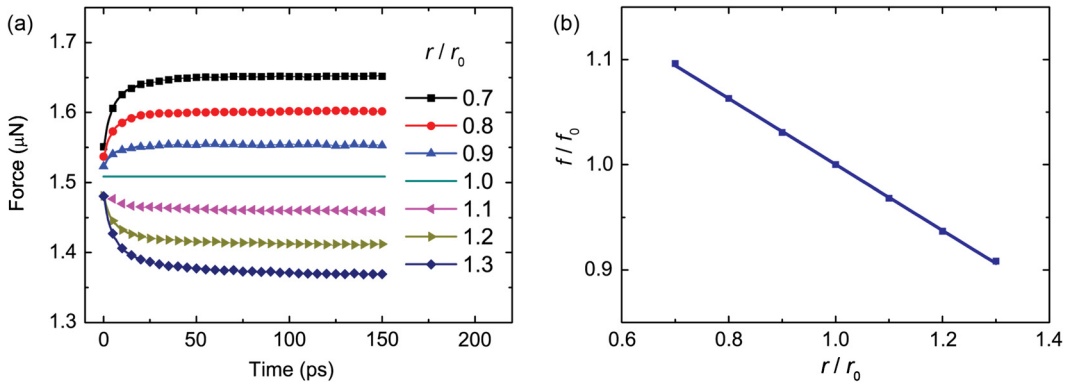

Fig. 4. (Color online.) (a) Responses in the tensile force at a pre-strain of 0.25, when the crosslink length is modified from r_0 to r. (b) Responses in the tensile force measured as a function of the change in the crosslink length r/r_0 that is fitted to the generalized Kelvin–Voigt model.

$$m\ddot{x} + c\dot{x} + k_{\text{eff}}x = 0 \tag{3}$$

where m and c are the effective mass and damping coefficients. The solution of Eq. (3) shows a damped oscillation with force amplitude $f = k_{\text{eff}}x = A\exp(-\xi\omega t)\sin(\omega t + B)$, where A and B are constants defined by the initial conditions. The oscillating behavior in response is modulated from the underdamping to the overdamping regime, with the following critical damping condition:

$$\xi = \frac{c}{2\sqrt{mk_{\text{eff}}}} \sim \sqrt{\frac{k_1 + k_2}{k_1 k_2}} \tag{4}$$

As a result, ξ increases when k_2 decreases, and the oscillation is removed in the underdamping regime, as observed in Fig. 2.

Length. Another tunable parameter of the crosslink is its equilibrium length r_0. When r_0 deviates from its value initially set, the potential energy of a crosslink increases. Stress relaxation thus occurs subsequently according to the adjustment of the network microstructures. For each modified value of r_0 from 1.0 nm to a value between 0.7 and 1.3 nm, a duration of ~20 ps is required for the system to recover to a stable state, as shown in Fig. 4a. Then the amplitude of the force saturates into a constant f. The response in force amplitude f/f_0 is plotted in Fig. 4b as a function of the relative length scaling factor r/r_0, which suggests a linear dependence between them, i.e. f/f_0 decreases as r/r_0 increases. This result is in contrast to the relatively magnified response when softening the crosslink by decreasing k.

This dependence could also be explained by the generalized Kelvin–Voigt model. Solving Eq. (1) gives:

$$f = k_{\text{eff}}L\left[\varepsilon_0 + \beta(r_0 - r)/r\right] \tag{5}$$

where k_{eff} is the stiffness of the whole system, β is a fitting parameter introduced to include the contribution of a single crosslink to the strain. Fitting the simulation results in Fig. 4 yields $\beta = 0.078$, and the stiffness of the material is 50.2 N/m compared to 34.3 N/m as obtained above from our simulations with a modified stiffness of the crosslinks. In addition, the time scale of the relaxation is predicted by $\tau = (\eta_1 + \eta_2)/(k_1 + k_2)$, depending synergetically on both the CNT network and crosslinks. According to this formula, τ decreases when k_2 increases as shown in Fig. 2, but does not change with r (Fig. 4a).

3.2.2. *Responses in a pre-stressed network*

Similar effects have also been observed while a pre-stress is applied, as illustrated by the results plotted in Figs. 5a and 5b. The pre-tension in the simulations is $f_0 = 2.7$ μN. Softening shows a more prominent effect in the response. By tuning the stiffness of crosslinks from $k_0 = 10$ N/m to values in the range of 1–1000 N/m, we fit the response in strain amplitude by:

$$\varepsilon = f_0(1/k_1 + 1/k_2)/L \tag{6}$$

where $k_2 = \gamma k$, with k the modified stiffness of a single crosslink as defined above. The fitting parameters γ and the stiffness of CNTs k_1 are 57.1 and 45.9 N/m, respectively. These fitting results are consistent with the value $k_1 = 80$ N/m obtained above, with quantitative deviation due to the simplified nature of our analytical model. Numerical fitting using parameters γ and k_1 is also plotted in Fig. 5b. The consistence further validates the predictability of the model. The typical relaxation time is $\tau = \eta_2/k_2$. Thus, as k_2 increases, the time scale of the relaxation τ decreases. However, it does not change with r. Thus the mechanical response at the network level can be modulated by molecular-level crosslinks in both pre-strain and pre-stress boundary conditions, and is expected to be valid in their combination as well.

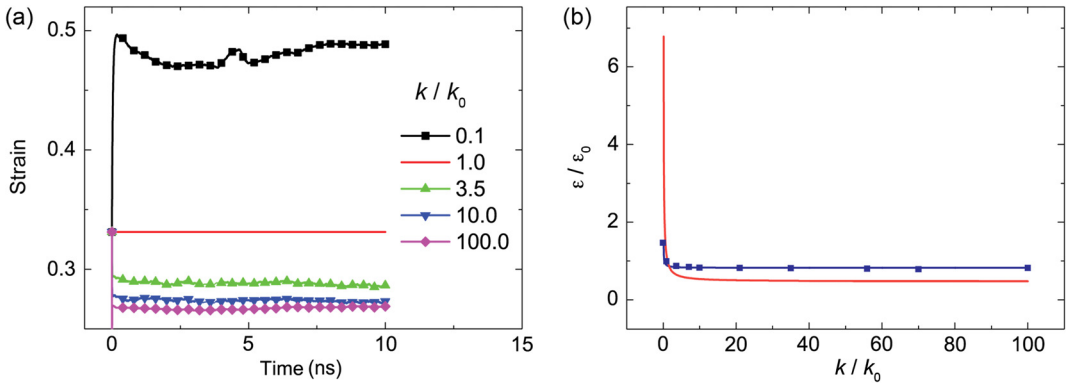

Fig. 5. (Color online.) (a) Responses in the tensile strain at a pre-tension of 1.5 μN, when the stiffness of a single crosslink is modified from k_0 to k. (b) Responses in the tensile strain measured as a function of the change in the crosslink stiffness k/k_0. The red line corresponds to the prediction using the parameters fitting our prestrain results, as discussed earlier.

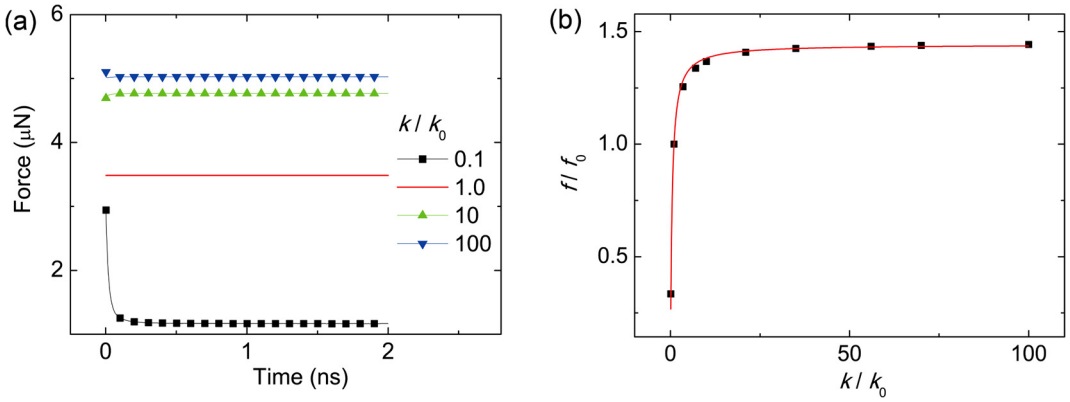

Fig. 6. (Color online.) (a) Response under equibiaxial loading with a pre-strain of 0.25, when the crosslink's stiffness is modified from k_0 to k. (b) Response in tensile force f/f_0 measured as a function of the stiffening factor k/k_0.

3.2.3. Responses under biaxial loading conditions

We further extend our exploration to equibiaxial loading conditions. The results show effects similar to the simulation results for uniaxial loading conditions shown above. For the pre-strain condition with an initial strain of 0.25, the tension force in one direction was measured after the crosslinks' stiffness was tuned (Fig. 6a). The force increases as the crosslink becomes stiffer (Fig. 6b). Eq. (2) also fits well the simulation results and the fitting parameters of network stiffness k_1 and α are 167.6 N/m and 38.2, respectively. Compared to the uniaxial loading conditions, the response in force is more prompt here because a more affined deformation could be realized under biaxial loads as the reorientation of CNTs is avoided [13]. With a pre-tension f_0 of 3.5 μN, the strain in both directions was measured (Fig. 7a). The fitting parameters γ and the stiffness of CNTs k_1 using Eq. (6) are 41.9 and 134.7 N/m, respectively (Fig. 7b). The latter value is consistent with that of 167.6 N/m with biaxial pre-strain.

4. Discussion

The generalized Kelvin–Voigt model constructed here offers a minimal consideration of the mechanical response to crosslink stiffness and length modulation. However, limited for the sake of simplification to the use of only two units, the fitted parameters from our pre-stress and pre-strain simulations yield quantitatively different, although reasonably consistent, results. The variation in network microstructures upon different loading conditions as encountered in the simulations, as well as the randomness in network structures and crosslinks, could lead to additional sources of the deviation of fitting parameters in the model. To improve the model and extend the understanding for material optimization, a continuum-level viscoelastic model may help.

5. Conclusion

To conclude, we explored the responsive mechanics of crosslinked fiber-network materials using CNTs as an example here. By functionalizing CNTs on their sidewalls or ends, various chemical groups could be introduced, and the interactions between CNTs through these binding agents can be engineered [25]. Coarse-grained molecular dynamics simulation

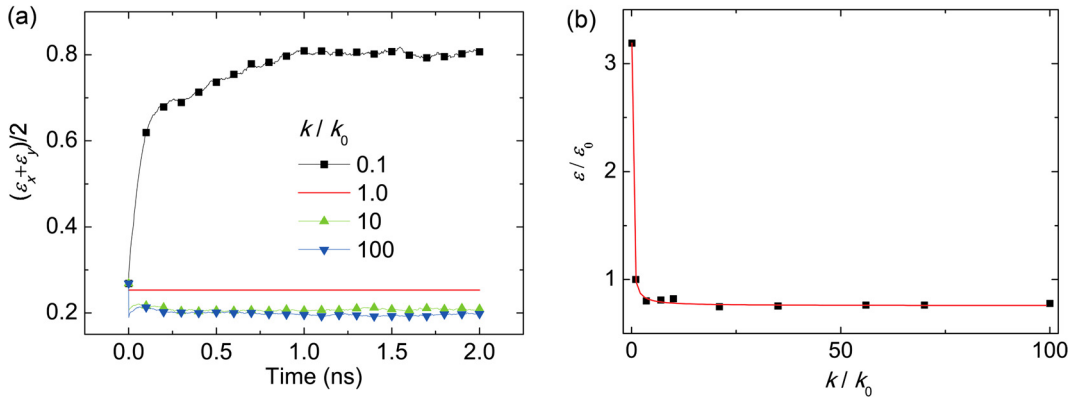

Fig. 7. (Color online.) (a) Response in equibiaxial loading at a pre-tension of 3.5 μN, when the stiffness of a single crosslink is modified from k_0 to k. (b) Response in tensile strain measured as a function of the change in the crosslink stiffness k/k_0.

and analysis results reveal not only the dependence of the response on controlling parameters, the stiffness and length of crosslinks, but also the detailed microscale dynamics. The prompt response in a subnanosecond timescale and the predicted dependence of the mechanical behavior on the crosslinking nature and its changes imply their high performance as responsive materials.

In this work, random fiber networks are investigated. However, the performance could be further enhanced by using more regular, woven structures. Two further important issues, the dynamic responses of the network material at finite frequency [18], and effects of the medium (e.g., hydrated environment, polymer matrix), are not discussed here, but in principle could be studied using the techniques introduced here.

Acknowledgements

This work was supported by the National Natural Science Foundation of China through Grants 11222217, 11002079, Tsinghua University Initiative Scientific Research Program 2011Z02174. L.F. Wang acknowledges the support of the National Science Foundation under Award number CMMI-1234768. The computation was performed on the Explorer 100 cluster system of Tsinghua National Laboratory for Information Science and Technology.

References

[1] R. Lakes, Materials with structural hierarchy, Nature 361 (1993) 511.
[2] M.J. Buehler, Y.C. Yung, Deformation and failure of protein materials in physiologically extreme conditions and disease, Nat. Mater. 8 (2009) 175.
[3] N. Halonen, A. Rautio, A.-R. Leino, T. Kyllönen, G. Tóth, J. Lappalainen, K. Kordás, M. Huuhtanen, R.L. Keiski, A. Sápi, M. Szabó, A. Kukovecz, Z. Kónya, I. Kiricsi, P.M. Ajayan, R. Vajtai, Three-dimensional carbon nanotube scaffolds as particulate filters and catalyst support membranes, ACS Nano 4 (2010) 2003.
[4] F. Deng, M. Ito, T. Noguchi, L. Wang, H. Ueki, K.-i. Niihara, Y.A. Kim, M. Endo, Q.-S. Zheng, Elucidation of the reinforcing mechanism in carbon nanotube/rubber nanocomposites, ACS Nano 5 (2011) 3858.
[5] K.E. Kasza, A.C. Rowat, J. Liu, T.E. Angelini, C.P. Brangwynne, G.H. Koenderink, D.A. Weitz, The cell as a material, Curr. Opin. Cell Biol. 19 (2007) 101.
[6] S.W. Cranford, A. Tarakanova, N.M. Pugno, M.J. Buehler, Nonlinear material behaviour of spider silk yields robust webs, Nature 482 (2012) 72.
[7] J.S. Mohammed, W.L. Murphy, Bioinspired design of dynamic materials, Adv. Mater. 21 (2009) 2361.
[8] M.A.C. Stuart, W.T.S. Huck, J. Genzer, M. Muller, C. Ober, M. Stamm, G.B. Sukhorukov, I. Szleifer, V.V. Tsukruk, M. Urban, F. Winnik, S. Zauscher, I. Luzinov, S. Minko, Emerging applications of stimuli-responsive polymer materials, Nat. Mater. 9 (2010) 101.
[9] R.J. Wojtecki, M.A. Meador, S.J. Rowan, Using the dynamic bond to access macroscopically responsive structurally dynamic polymers, Nat. Mater. 10 (2011) 14.
[10] N. Holten-Andersen, M.J. Harrington, H. Birkedal, B.P. Lee, P.B. Messersmith, K.Y.C. Lee, J.H. Waite, pH-induced metal–ligand cross-links inspired by mussel yield self-healing polymer networks with near-covalent elastic moduli, Proc. Natl. Acad. Sci. USA 108 (2011) 2651.
[11] D.E. Fullenkamp, L. He, D.G. Barrett, W.R. Burghardt, P.B. Messersmith, Mussel-inspired histidine-based transient network metal coordination hydrogels, Macromolecules 46 (2013) 1167.
[12] H. Xu, J. Nishida, W. Ma, H. Wu, M. Kobayashi, H. Otsuka, A. Takahara, Competition between oxidation and coordination in cross-linking of polystyrene copolymer containing catechol groups, ACS Macro Lett. 1 (2012) 457.
[13] B. Xie, Y. Liu, Y. Ding, Q. Zheng, Z. Xu, Mechanics of carbon nanotube networks: microstructural evolution and optimal design, Soft Matter 7 (2011) 10039.
[14] C. Wang, B. Xie, Y. Liu, Z. Xu, Mechanotunable microstructures of carbon nanotube networks, ACS Macro Lett. 1 (2012) 1176.
[15] N. Fakhri, D.A. Tsyboulski, L. Cognet, R.B. Weisman, M. Pasquali, Diameter-dependent bending dynamics of single-walled carbon nanotubes in liquids, Proc. Natl. Acad. Sci. USA 106 (2009) 14219.
[16] F.C. MacKintosh, J. Käs, P.A. Janmey, Elasticity of semiflexible biopolymer networks, Phys. Rev. Lett. 75 (1995) 4425.
[17] C.P. Broedersz, M. Depken, N.Y. Yao, M.R. Pollak, D.A. Weitz, F.C. MacKintosh, Cross-link-governed dynamics of biopolymer networks, Phys. Rev. Lett. 105 (2010) 238101.
[18] T.B. Liverpool, M.C. Marchetti, J.F. Joanny, J. Prost, Mechanical response of active gels, Europhys. Lett. 85 (2009) 18007.
[19] Z. Xu, Mechanics of metal–catecholate complexes: the roles of coordination state and metal types, Sci. Rep. 3 (2013) 2914.
[20] S. Cranford, M.J. Buehler, In silico assembly and nanomechanical characterization of carbon nanotube buckypaper, Nanotechnology 21 (2010) 265706.

[21] Y. Liu, B. Xie, Z. Xu, Mechanics of coordinative crosslinks in graphene nanocomposites: a first-principles study, J. Mater. Chem. 21 (2011) 6707.
[22] M. Xu, D.N. Futaba, T. Yamada, M. Yumura, K. Hata, Carbon nanotubes with temperature-invariant viscoelasticity from −196 °C to 1000 °C, Science 330 (2010) 1364.
[23] R.L.D. Whitby, T. Fukuda, T. Maekawa, S.L. James, S.V. Mikhalovsky, Geometric control and tuneable pore size distribution of buckypaper and buckydiscs, Carbon 46 (2008) 949.
[24] B. Ashrafi, J. Guan, V. Mirjalili, P. Hubert, B. Simard, A. Johnston, Correlation between Young's modulus and impregnation quality of epoxy-impregnated SWCNT buckypaper, Composites, Part A, Appl. Sci. Manuf. 41 (2010) 1184.
[25] S. Acquah, D. Ventura, H. Kroto, in: J.M. Marulanda (Ed.), Electronic Properties of Carbon Nanotubes, Intech, 2011.